# Electronic Supplementary Information

## Experimental Section

**Materials:** Ti mesh was provided by Hangxu Filters Flag Store, Hengshui, Hebei. $NH_4F$, NaOH, $KH_2PO_4$, and $K_2HPO_4$ were purchased from Beijing Chemical Corp. $RuCl_3 \cdot 3H_2O$, $Co(NO_3)_2 \cdot 6H_2O$ and urea were purchased from Aladdin Ltd. (Shanghai, China). Nafion (5 wt%) was purchased from Sigma-Aldrich. All the reagents were used as received. The water used throughout all experiments was purified through a Millipore system.

**Preparation of $Co(CO_3)_{0.5}(OH)0.11H_2O$ nanoarray on Ti mesh (CCH NA/Ti):** A piece of Ti mesh (2 cm × 3 cm) was carefully pre-treated with concentrated HCl for 10 minutes to remove impurity of surface, and then deionized water and ethanol were used for several times to ensure the surface of the Ti mesh was well cleaned. After drying, the weight of each treated Ti mesh was recorded. Synthesis of hydroxide precursor, 3 mmol of $Co(NO_3)_2 \cdot 6H_2O$, 8 mmol of $NH_4F$, and 15 mmol of urea were dissolved in 50 mL deionized water to form a transparent pink solution by constant stirring. Then the solution was transferred into a 50 mL polytetrafluoro-ethylene Teflon-lined stainless steel autoclave. The pre-treated Ti mesh was immersed in the solution, sealed and kept at 120 °C for 6 h. The loading of carbonate hydroxide was calculated to be 2.4 mg $cm^{-2}$ by measuring the weight difference of Ti substrate before and after the hydrothermal process.

**Preparation of CCH@Co-Pi NA/Ti**: To obtain CCH@Co-Pi NA/Ti, the CCH NA/Ti electrode as the working electrode was polarized at 1.6 V (vs. Ag/AgCl) in 0.1 M PBS (pH 7) until the current density reaches a plateau, with the use of Pt wire as the auxiliary electrode and a Ag/AgCl as the reference electrode.

**Synthesis of $RuO_2$:** Typically, 0.01 mol of $RuCl_3 \cdot 3H_2O$ was added into 100 mL distilled water, and NaOH (1.0 M) was added to adjust the pH to 7. The mixed solution was stirred for 45 min at 100 °C and then centrifuged for 10 minutes and filtered. The precipitate was collected and washed with water several times. Finally, the product was dried at 80 °C overnight and then annealed at 350 °C in air for 1 h.

The as-prepared $RuO_2$ powder (0.04 g) was dispersed into a solution of Nafion, ethanol and water with a volume ratio of 20/480/500 via sonication, and deposited onto Ti mesh with a loading of 2.4 mg $cm^{-2}$.

**Electrochemical measurements:** Electrochemical measurements were performed with a CHI 660E electrochemical analyzer (CH Instruments, Inc., Shanghai) in a conventional three-electrode system where the reference electrode was Ag/AgCl (3 M KCl). CCH@Co-Pi NA/Ti and Pt wire were used as counter and working electrodes respectively. Overpotentials ($\eta$) were calculated by the following equation: $\eta$ = E (RHE) – 1.23 V, where E (RHE) = E (Ag/AgCl) + (0.197 + 0.059 pH) V. Polarization curves were obtained using linear sweep voltammetry with a scan rate of 2 mV $s^{-1}$ in 0.1 M PBS electrolyte. All experiments were carried out at room temperature (298 K).

**Characterizations:** Powder X-ray powder diffraction (XRD) data of the samples were collected on Bruker D8 ADVANCE Diffractiometer ($\lambda$=1.5418 Å). The scanning electron microscopy (SEM) measurements were performed on a XL30 ESEM FEG scanning electron microscope at an accelerating voltage of 20 kV. Transmission electron microscopy (TEM) measurements were performed on a HITACHI H-8100 electron microscopy (Hitachi, Tokyo, Japan) with an accelerating voltage of 200 kV. X-ray photoelectron spectroscopy (XPS) measurements were collected with a Thermal ESCALAB 250 spectrometer using an Al Kα X-ray source (1486.6 eV photons).

**Double layer capacitance ($C_{dl}$) measurements:** To measure the electrochemical capacitance, the potential was swept between 0.81 to 0.91 V five times at each of eleven different scan rates (20, 60, 120,180, 250, and 300 mV $s^{-1}$) with an assumption that double layer charging in the potential range. The capacitive currents at 0.86 V were measured and plotted as a function of scan rate. A linear fit determined the double layer capacitance to be 194 μF $cm^{-2}$.

**Turn over frequency (TOF) calculations:** The TOF ($s^{-1}$) was calculated following equation:

$$TOF = \frac{I}{4nF}$$

Here $I$ is current (A) during the LSV measurement in 0.1 M PBS, $F$ is the Faradic constant (96485 C mol$^{-1}$) and $n$ is the number of cobalt atoms, which is calculated by the loading of $Co(CO_3)_{0.5}(OH)0.11H_2O$.

**Determination of Faradaic efficiency (FE):** Under the oxidative conditions, quantitative oxygen production experiments were performed with the CCH@Co-Pi NA/Ti as the working electrode. The generated gas was confirmed by gas chromatography (GC) analysis and measured quantitatively using a calibrated pressure sensor to monitor the pressure change in the cathode compartment of an H-type electrolytic cell. The moles of oxygen was calculated by the equation of PV= nRT, where V is stable for the equipment, R is 8.314 J mol$^{-1}$ K$^{-1}$ and T is 298 K. The theoretical amount of oxygen was calculated by assuming that all charges that passed through the working electrode were 4e$^-$ oxidation of water by Faraday's Law.

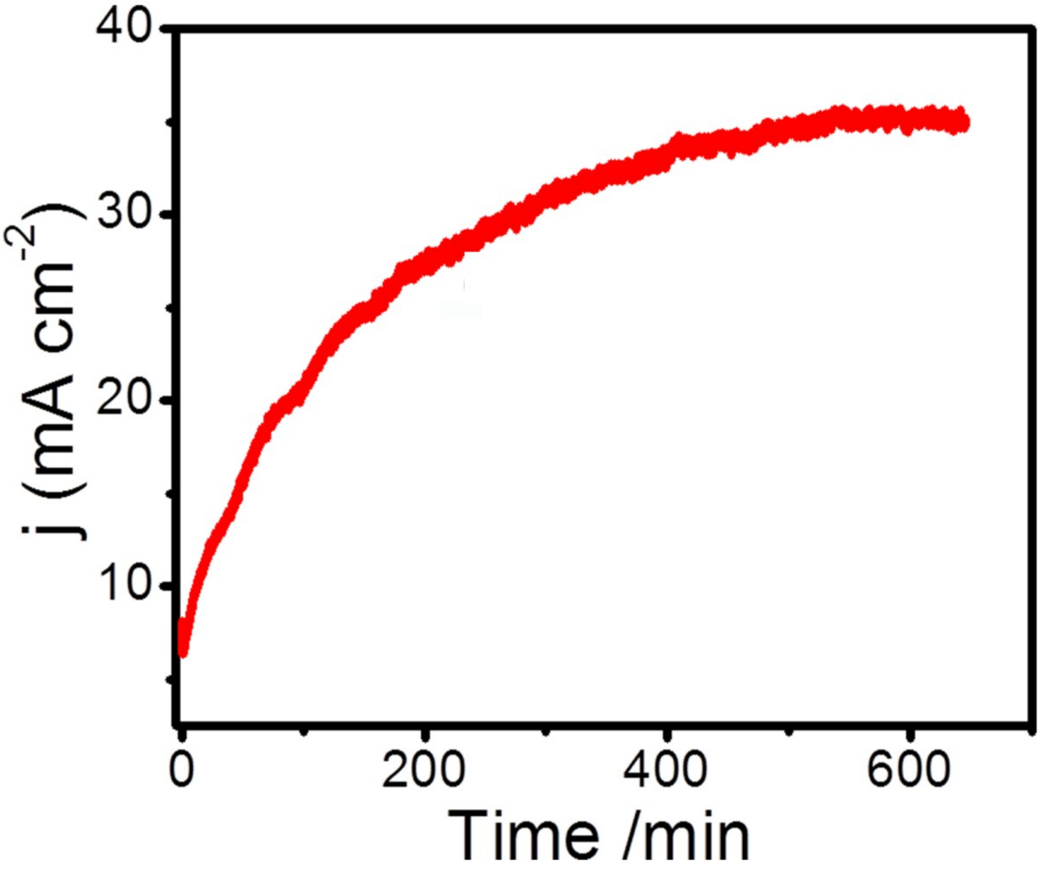

**Fig. S1** Current density trace for CCH NA/Ti at 1.6 V (vs. Ag/AgCl) in 0.1 M PBS (pH 7.0).

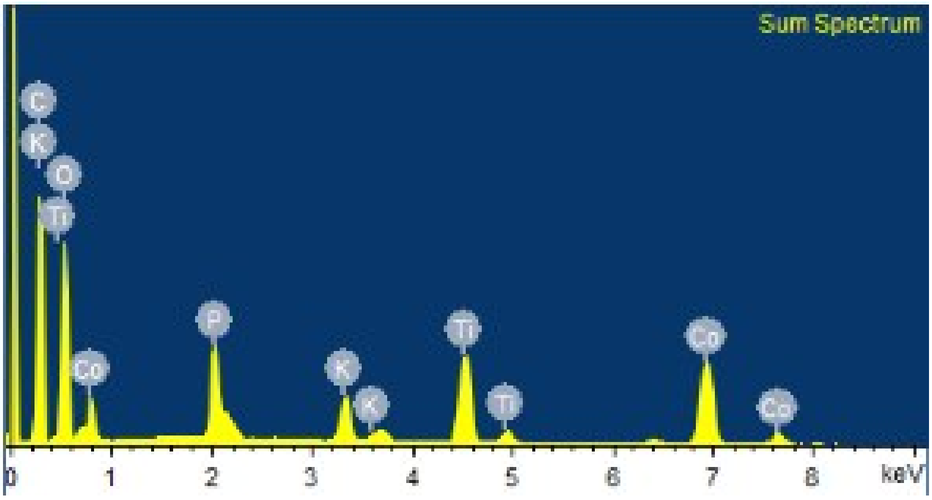

**Fig. S2** EDX spectrum of CCH@Co-Pi NA/Ti.

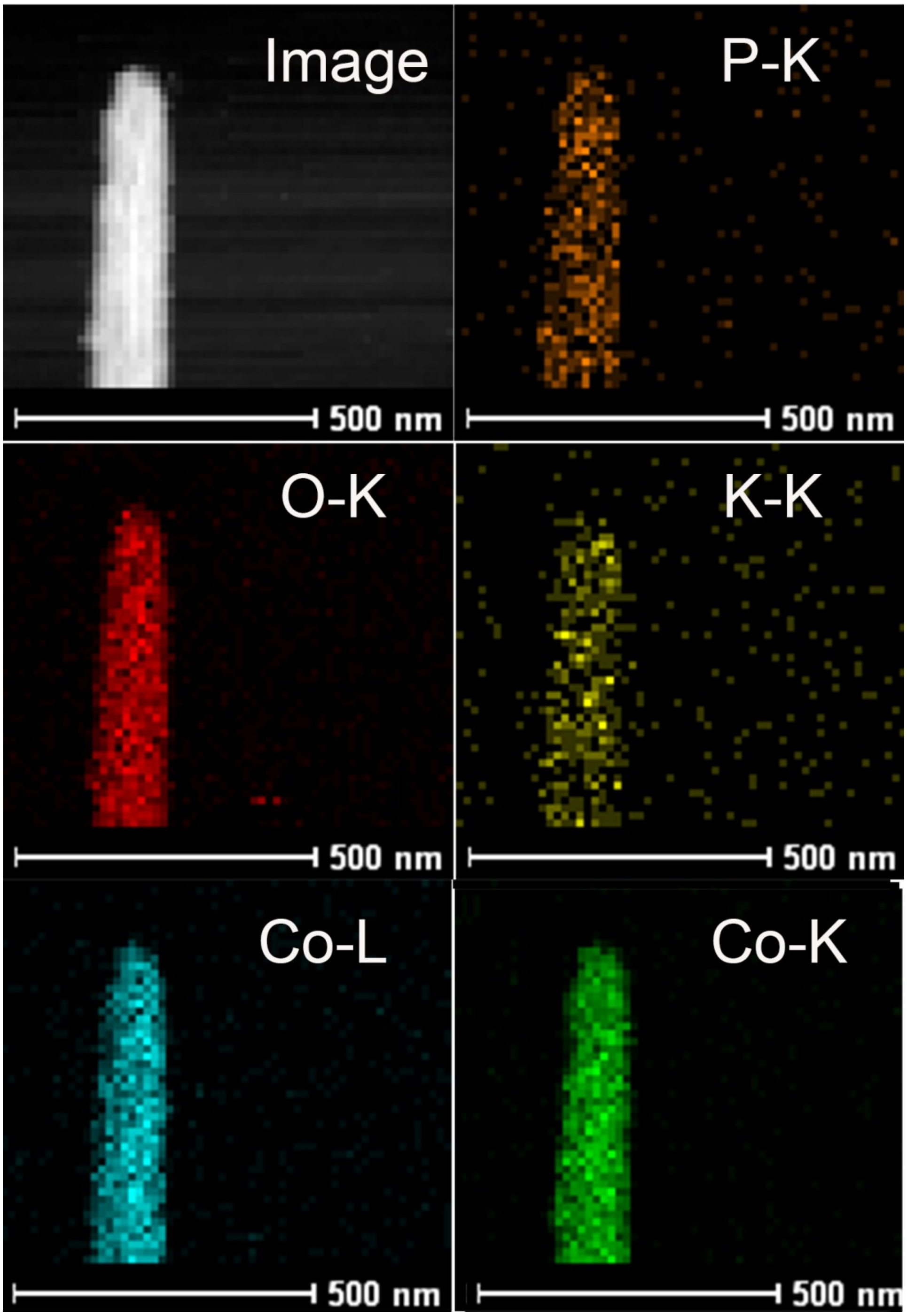

**Fig. S3** Scanning TEM (STEM) image and EDX elemental mapping of P, O, K and Co for a CCH@Co-Pi core@shell nanowire.

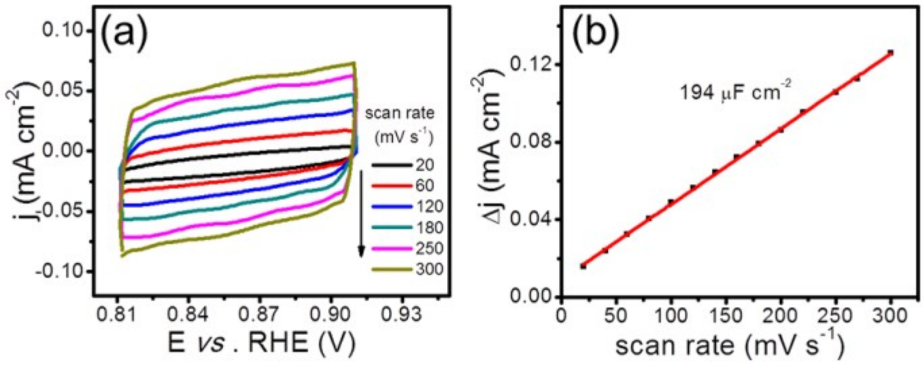

**Fig. S4** (a) Cyclic voltammograms for CCH@Co-Pi NA/Ti in the non-faradaic capacitance current range at scan rates of 20, 60, 120,180, 250, and 300 mV $s^{-1}$.(b) The capacitive currents at 0.86 V as a function of scan rate for CCH @Co-Pi NA/Ti.

**Table S1** Comparison of OER performance for CCH@Co-Pi NA/Ti with other non-noble-metal OER electrocatalysts in PBS electrolyte.

| Catalyst | j (mA cm$^{-2}$) | $\eta$ (mV) | PBS concentration | Ref. |
|---|---|---|---|---|
| Co-Pi NA/Ti | 5 | 357 | 0.1 M | This work |
| | 10 | 460 | | |
| | 10 | 430 | 0.5 M | |
| | 100 | 670 | 1.0 M | |
| Co-Pi/ITO | 1 | 410 | 0.1 M | 1 |
| Co-Pi/ITO | 1 | 483 | 0.1 M | 2 |
| Co-Pi/FTO | 0.43 | 420 | 0.1 M | 3 |
| Co-Pi film | 0.63 | 483 | 0.1 M | 4 |
| CoPi/GO | 0.23 | 780 | 0.1 M | 5 |
| Co-OEC/Ni foam | 100 | 442 | 1.0 M | 6 |
| $Co(PO_3)_2$ | 10 | 590 | 0.1 M | 7 |
| $Co_3S_4$ | 3 | 620 | 0.1 M | 8 |
| $Li_2Co_2O_4$ | 1 | 545 | 0.1 M | 9 |
| Co-Ni LDH | 1 | 490 | 0.1 M | 10 |
| $Co_3O_4$/MWNTs | 1 | 400 | 0.1 M | 11 |
| CoCat | 1 | 813 | 0.1 M | 12 |
| Co-W | 1 | 420 | 0.05 M | 13 |
| $Co(OH)_2$ | 1 | 710 | 0.1 M | 14 |
| CoHCF | 1 | 580 | 0.05 M | 15 |
| $Co_3O_4$ nanorod | 1 | 385 | 0.1 M | 16 |
| NGCO | 1 | 410 | 0.1 M | 17 |
| Fe-based film | 1 | 480 | 0.1 M | 18 |
| Ni-Gly | 1 | 480 | 0.5 M | 19 |
| $MnO_x$ | 1 | 580 | 0.1 M | 20 |

| | | | | |
|---|---|---|---|---|
| Sub-$MnO_x$ | 1 | 420 | 0.3 M | 21 |
| Cu-doped CCO | 1 | 653 | 0.1 M | 22 |
| $Mn_5O_8$ | 5 | 580 | 0.3 M | 23 |
| $Mn_3(PO_4)_2$ | 0.32 | 680 | 0.5 M | 24 |
| $LiMnP_2O_7$ | 0.5 | 680 | 0.5 M | 25 |

## References

1 M. W. Kanan and D. G. Nocera, *Science* **2008**, *312*, 1072–1075.

2 Y. Surendranath, M. Dinca and D. G. Nocera, *J. Am. Chem. Soc.* **2009**, *131*, 2615–2620.

3 E. R. Young, D. G. Nocera and V. Bulović, *Energy Environ. Sci.* **2010**, *3*, 1726–1728.

4 M. W. Kanan, J. Yano, Y. Surendranath, M. Dincă, V. K. Yachandra and D. G. Nocera, *J. Am. Chem. Soc.* **2010**, *132*, 13692–13701.

5 A. Vasileff, S. Chen and S. Qiao, *Nanoscale Horiz.* **2016**, *1*, 41–44.

6 A. J. Esswein, Y. Surendranath, S. Y. Reece and D. G. Nocera, *Energy Environ. Sci.* **2011**, *4*, 499–504.

7 H. S. Ahn and T. D. Tilley, *Adv. Funct. Mater.* **2013**, *23*, 227–233.

8 Y. Liu, C. Xiao, M. Lyu, Y. Lin, W. Cai, P. Huang, W. Tong, Y. Zou and Y. Xie, *Angew. Chem. Int. Ed.* **2015**, *54*, 11231–11235.

9 G. P. Gardner, Y. B. Go, D. M. Robinson, P. F. Smith, J. Hadermann, A. Abakumov, M. Greenblatt and G. C. Dismukes, *Angew. Chem. Int. Ed.* **2012**, *51*, 1616–1619.

10 Y. Zhang, B. Cui, C. Zhao, H. Lin and J. Li, *Phys. Chem. Chem. Phys.* **2013**, *15*, 7363–7369.

11 J. Wu, Y. Xue, X. Yan, W. Yan, Q. Cheng and Y. Xie, *Nano Res.* **2012**, *5*, 521–530.

12 D. González-Flores, I. Sánchez, I. Zaharieva, K. Klingan, J. Heidkamp, P. Chernev, P. W. Menezes, M. Driess, H. Dau and M. L. Montero, *Angew. Chem. Int. Ed.* **2015**, *54*, 2472–2476.

13 Y. Zhang, B. Cui, O. Derr, Z. Yao, Z. Qin, X. Deng, J. Li and H. Lin, *Nanoscale* **2014**, *6*, 3376–3383.

14 B. Zhang, X. Wu, F. Li, F. Yu, Y. Wang and L. Sun, *Chem. Asian J.* **2015**, *10*, 2228–2233.

15 Y. Zhang, B. Cui, Z. Qin, H. Lin and J. Li, *Nanoscale* **2013**, *5*, 6826–6833.

16 S. Pintado, S. Goberna-Ferron, E. C. Escudero-Adan and J. R. Galán-Mascarós *J. Am. Chem. Soc*. **2013**, *135*, 13270–13273.

17 R. M. Ramsundar, J. Debgupta, V. K. Pillai and P. A. Joy, *Electrocatal.* **2015**, *6*, 331–340.

18 J. Tian, H. Li, A. M. Asiri, A. O. Al-Youbi and X. Sun, *Small* **2013**, *9*, 2709–2714.

19 Y. Wu, M. Chen, Y. Han, H. Luo, X. Su, M. Zhang, X. Lin, J. Sun, L. Wang, L. Deng, W. Zhang and R. Cao, *Angew. Chem. Int. Ed.* **2015**, *54*, 4870–4875.

20 D. Jeong, K. Jin, S. E. Jerng, H. Seo, D. Kim, S. H. Nahm, S. H. Kim and K. T. Nam, *ACS Catal.* **2015**, *5*, 4624–4628.

21 I. Zaharieva, P. Chernev, M. Risch, K. Klingan, M. Kohlhoff, A. Fischer and H. Dau, *Energy Environ. Sci.* **2012**, *5*, 7081–7089.

22 J. Park, H. Kim, K. Jin, B. J. Lee, Y. S. Park, H. Kim, I. Park, K. D. Yang, H. Y. Jeong, J. Kim, K. T. Hong, H. W. Jang, K. Kang and K. T. Nam, *J. Am. Chem. Soc.* **2014**, *136*, 4201–4211.

23 D. Wang, G. Ghirlanda and J. P. Allen, *J. Am. Chem. Soc.* **2014**, *136*, 10198–10201.

24 K. Jin, A. Chu, J. Park, D. Jeong, S. E. Jerng, U. Sim, H. Y. Jeong, C. W. Lee, Y. S. Park, K. D. Yang, G. K. Pradhan, D. Kim, N. E. Sung, S. H. Kim and K. T. Nam, *Sci. Rep.* **2015**, *5*, 10279.

25 K. Jin, J. Park, J. Lee, K. D. Yang, G. K. Pradhan, U. Sim, D. Jeong, H. L. Jang, S. Park, D. Kim, N. E. Sung, S. H. Kim, S. Han and K. T. Nam, *J. Am. Chem. Soc.* **2014**, *136*, 7435–7443.